Journal of the European Ceramic Society 22 (2002) 2555–2560

www.elsevier.com/locate/jeurceramsoc

High-temperature deformation of a $BaCe_{0.8}Y_{0.2}O_{3-y}$ + Ni composite

A.R. de Arellano-Lopez[a], K.C. Goretta[b], E.T. Park[b], S.E. Dorris[b], U. Balchandran[b], J.L. Routbort[b,*]

[a]*Department of Condensed Matter Physics, University of Sevilla, PO Box 1065, Seville, Spain*
[b]*Argonne National Laboratory, Energy Technology Division, 9700 South Cass Avenue, Argonne, IL 60439-4838 USA*

Received 20 October 2001; received in revised form 27 February 2002; accepted 15 March 2002

Abstract

Steady-state compressive creep experiments have been performed on a 60 vol.% $BaCe_{0.8}Y_{0.2}O_{3-y}$/40 vol.% Ni composite in the temperature range of 1100–1370 °C at stresses of 2–150 MPa. The addition of Ni to $BaCe_{0.8}Y_{0.2}O_{3-y}$ increases the creep rate compared to $BaCe_{0.8}Y_{0.2}O_{3-y}$ without Ni. The composite creep response is modeled on the basis of hard grains ($BaCe_{0.8}Y_{0.2}O_{3-y}$) surrounded by the soft Ni phase.

Keywords: Deformation; Creep; Membrane; Perovskite; Ceramic–metal composite; Threshold stress

1. Introduction

Doped $BaCeO_3$ perovskites exhibit high proton and oxygen-ion conductivity, high electronic conductivity, and reasonable chemical stability over a wide range of temperature and oxygen partial pressure $p(O_2)$.[1–9] As a result they are receiving considerable attention as membranes, as evidenced by many reports on the defect chemistry, structure, conductivity, and processing of these materials.[1–17]

Two investigations on creep of these materials between 1200 and 1450 °C have been reported.[18,19] The conclusion was that compressive steady-state creep was the result of grain-boundary sliding (GBS) that was controlled by lattice diffusion of one of the cations. The stress exponent was found to be 1.1 ± 0.1, the activation energy was 343 ± 30 kJ/mol,[18] and the creep rate was independent of $p(O_2)$ from 0.1 to 2×10^4 Pa. No comprehensive defect model was proposed.

Recently, it was found that a composite of 60 vol.% $BaCe_{0.8}Y_{0.2}O_{3-y}$/40 vol.% Ni could serve as an improved membrane material[20] because of the higher electronic conductivity of Ni. It was therefore the objective of this work to investigate the high temperature creep properties of the composite and compare them to those of $BaCe_{0.8}Y_{0.2}O_{3-y}$.

2. Experimental methods

2.1. Sample preparation

$BaCe_{0.80}Y_{0.20}O_3$ (BCY) powder was prepared by mixing appropriate amounts of $BaCO_3$, CeO_2, and Y_2O_3 and calcining the mixture at 1000 °C for 12 h in air. This powder was then ball-milled and calcined again at 1200 °C for 10 h in air. After obtaining phase purity (judged by X-ray diffraction), the BCY powder was mixed with 40 vol.% nickel powder to increase its electronic conductivity. The powder mixture was then uniaxially pressed and sintered for 5 h at 1400–1450 °C in 4% H_2/balance Ar.[21] The density after sintering was 94% of theoretical density (7.25 g/cm^3) calculated from neutron diffraction data for BCY.[22] Test specimens of $3.5 \times 3.5 \times 5.5$ mm were cut from the sintered disk by a low-speed diamond saw. The compression faces (perpendicular to the long axis) were ground flat and parallel to within ± 10 μm. For comparison with the creep responses of BCY and the BCY + Ni composite, polycrystalline Ni was also deformed. Right parallelpipeds $6 \times 6 \times 10$ mm were cut from a commercial Ni 200 strip, and the surfaces were polished to be flat and parallel. The specimens were deformed in compression at various temperatures in Ar, with alumina platens placed between the pushrods and the Ni.[18]

* Corresponding author. Tel.: +1-603-252-5065; fax: +1-630-252-3604.

E-mail address: routbort@anl.gov (J.L. Routbort).

0955-2219/02/$ - see front matter
PII: S0955-2219(02)00116-4

2.2. Creep tests and microstructural studies

The composite specimens were compressed in high-purity Ar between Al_2O_3 platens at constant crosshead velocity, as was previously described;[18,19,23] Pt foil was used as a diffusion barrier. The temperature range was 1100–1370 °C and the approximate strain rate ($\dot{\varepsilon}$) range was 2×10^{-6} to 5×10^{-5} s^{-1}. No appreciable reaction between the Pt and the composite specimens was observed. Specimens were deformed until steady state was achieved. Steady-state stress (σ) was defined by a zero work-hardening rate[23,24] and was usually achieved within 2% strain. Microstructures of the as-sintered and deformed specimens were characterized by scanning electron microscopy (SEM). The specimens were prepared by conventional polishing techniques. Polished specimens were etched in dilute HNO_3 for ≈30 s to reveal grain boundaries.

3. Results

Creep results were initially plotted in the conventional manner, ln $\dot{\varepsilon}$ vs. ln σ in order to determine the deformation parameters in the Norton equation:

$$\dot{\varepsilon} = A\sigma^n \exp(-Q/RT), \quad (1)$$

where A is a constant, n is the stress exponent, R is the universal gas constant, T is the absolute temperature, and Q is the activation energy for creep. The activation energy can usually be related to the activation energy for diffusion of the rate-controlling species. However, when the data were plotted in this manner, the resulting stress exponent n varied systematically with temperature, with $n = 1.7$ at 1100 °C and $n = 1.3$ at 1370 °C. This result was surprising in light of the fact that the stress exponent for $BaCe_{0.8}Y_{0.2}O_{3-y}$ ($0.05 \leqslant \times \leqslant 0.2$) calculated from Eq. (1) was equal to 1, within experimental uncertainty.[18,19]

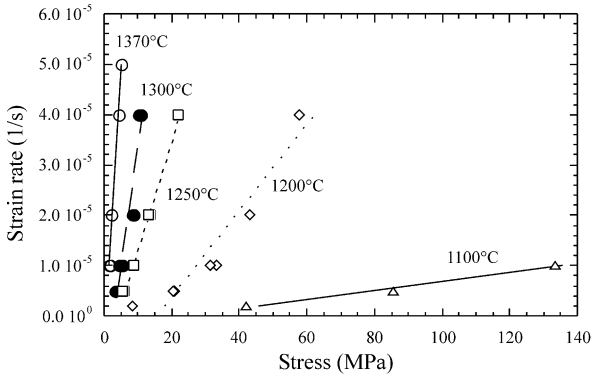

Fig. 1. Linear plot of strain rate vs. stress.

However, when the same results were plotted as $\dot{\varepsilon}$ vs. σ (Fig. 1), it became clear that the creep data could be fit to an equation of the form,

$$\dot{\varepsilon} = B(\sigma - \sigma_o)\exp(-Q/RT), \quad (2)$$

where σ_o is a threshold stress and B a constant. The correlation factors measured from the fits were between 0.94 and 1.0, quite close to unity. Such a linear plot indicated that the stress exponent was indeed unity, as shown in Fig. 2. The threshold stress depended on temperature, as shown in Fig. 3, having its highest value at the lowest temperature and approaching zero at the highest temperature.

Eq. 2 was used to calculate Q by plotting $\sigma - \sigma_o$ vs. $1/T$ for various $\dot{\varepsilon}$ (Fig. 4). Fits to the Arrhenius plot were very good, having correlation factors of ≈0.99. While there appeared to be some systematic dependence of the slopes (Q) with $\dot{\varepsilon}$, i.e. higher strain rates yielded lower activation energies, the average Q is 336±43 kJ/mol was in excellent accord with the previously reported results of 343±30 kJ/mol for creep of the BCY ceramic.[18]

When tested at the same temperatures and strain rates that were used for the BCY and the composite, the Ni exhibited serrated flow. The serrations were typical of those observed during creep of many face-centered cubic metals for which dynamic recrystallization occurs during deformation.[25] Because the Ni did not reach a true steady state, in order to compare the Ni data directly to those of the BCY, we have plotted the maximum flow stress of the Ni compared to the steady-state flow stress of the BCY. Under all test conditions, the Ni was substantially less creep resistant than was the BCY (Fig. 5).

The microstructure of an undeformed composite specimen was compared to one obtained after deformation

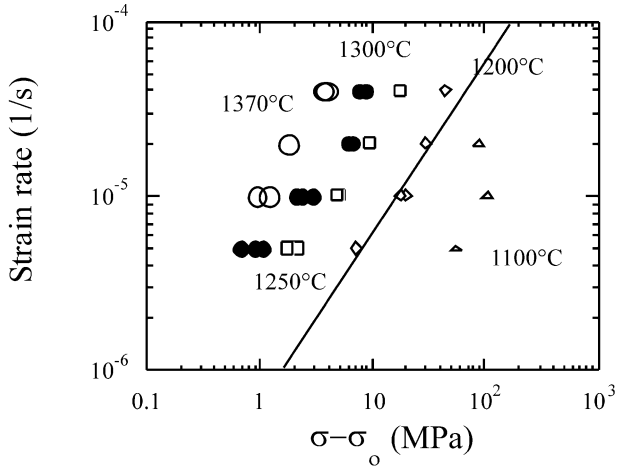

Fig. 2. Logarithmic plot of strain rate versus logarithm of (stress-threshold stress). The straight line is drawn with a slope of unity indicating the validity of the threshold stress concept.

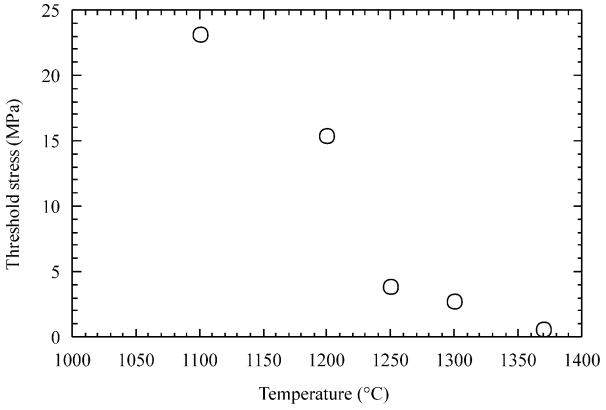

Fig. 3. Variation of the threshold stress with temperature.

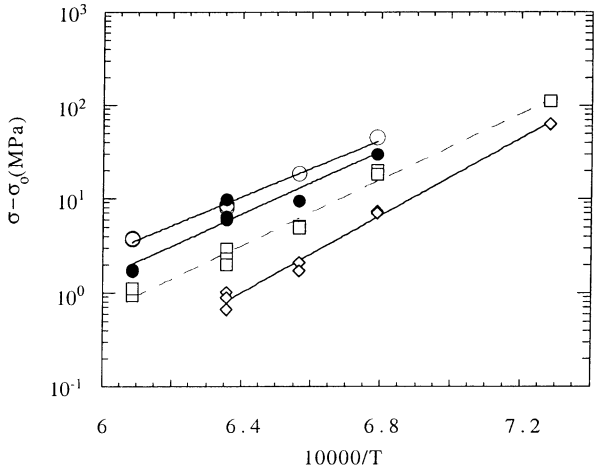

Fig. 4. Arrhenius plot of data for strain rates of 5×10^{-6} s^{-1} (diamonds), 1×10^{-5} s^{-1} (squares), 2×10^{-5} s^{-1} (solid circles), and 4×10^{-5} s^{-1} (open circles).

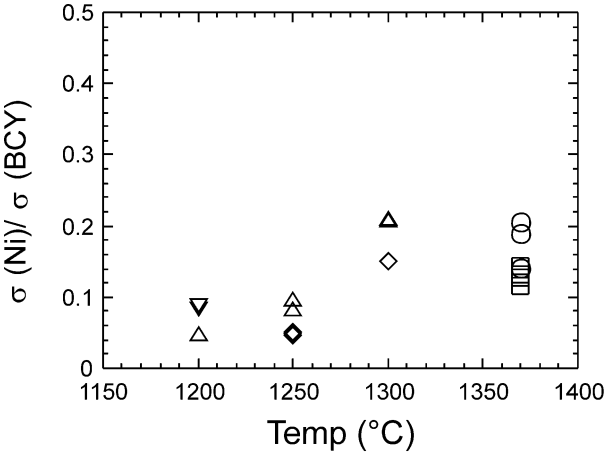

Fig. 5. Variation of the ratio of the steady-state stress of Ni 200 to that of the ceramic $BaCe_{0.8}Y_{0.2}O_{3-y}$. Symbols represent various strain rates: circles = 5 × 10–5 s^{-1}, squares = 4 × 10–5 s^{-1}, diamonds = 2 × 10–5 s^{-1}, triangles = 1 × 1–5 s^{-1}, and inverted triangles = 5 × 10–6 s^{-1}.

at 1370 °C to $\varepsilon = 0.2$ (Fig. 6). The SEM photomicrographs taken in the back-scattered mode indicated that there was little evidence of gross cavitation. Photomicrographs taken of etched undeformed and deformed specimen are shown in Fig. 7. The grain size of the ceramic phase remained relatively unchanged. The Ni phase (white in Fig. 6) recrystallized, as would be expected.[25]

4. Discussion

There are several important results to consider. Firstly, the addition of 40 vol.% of Ni to BCY results in a threshold stress for creep. If the threshold stress is taken into account, the stress exponent becomes unity and $Q \cong 336$ kJ/mol. Therefore, the composite and the ceramic have the same stress exponent and activation energy. It is tempting to suggest that the same mechanism, namely GBS, is the primary deformation mechanism in both materials. This is consistent with the fact that no grain shape change or cavitation occurred in the ceramic, at least up to $\varepsilon = 0.2$.

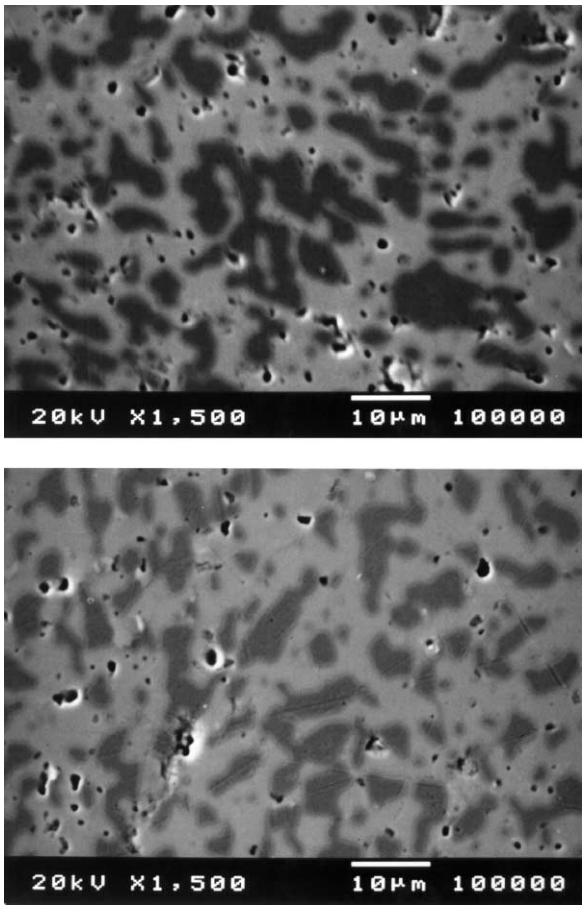

Fig. 6. SEM photomicrographs (backscattered mode) of undeformed (top) and sample deformed to 20% at 1370 °C (lower).

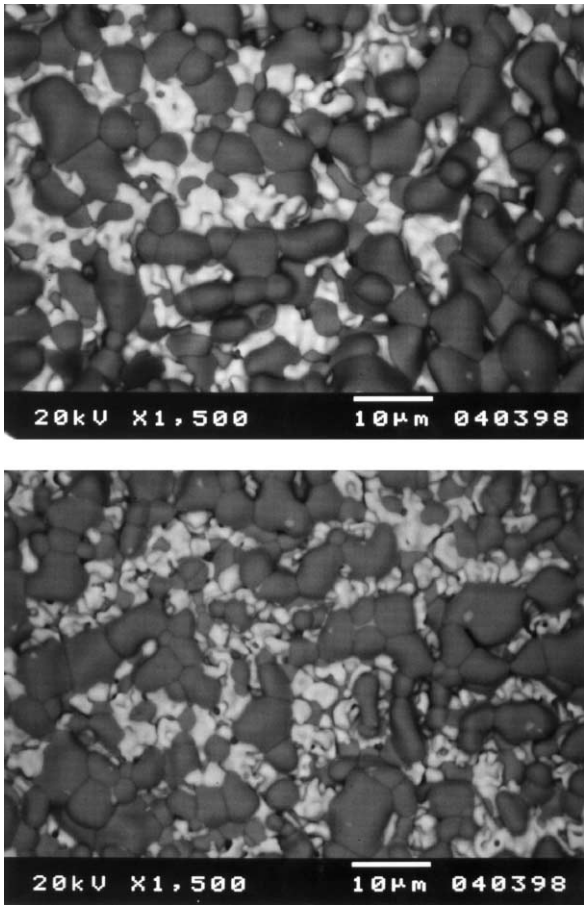

Fig. 7. SEM photomicrographs of an undeformed sample (top) and a specimen deformed to 20% at 1370 °C (bottom).

Constant-$\dot{\varepsilon}$ experiments on Ni 200 indicate that Ni is always softer than the ceramic (Fig. 5). While the ratio varies with $\dot{\varepsilon}$ and T, it is always considerably less than one. Therefore, $\dot{\varepsilon}$ of the composite, for a given stress, would expected to be greater than that of the pure ceramic. Fig. 8 shows a comparison of the creep rates of the ceramic and the composite. It is noted that the BCY grain sizes are approximately equal, 8 μm, so that a correction for grain size is unnecessary. The composite results are plotted as $\dot{\varepsilon}$ vs. $\sigma-\sigma_o$, while the BCY is plotted as $\dot{\varepsilon}$ vs. σ. As expected, the composite creeps faster than the ceramic: the enhancement factor for a given σ, $\dot{\varepsilon}_{composite}/\dot{\varepsilon}_{ceramic}$ is 8. If one assumes that the Ni phase contributes nothing to the stress, e.g., acts as if it were an interconnected pore, then the stress data for the composite should be corrected by $(1-p^{2/3})$, where p is the porosity.[26] This predicts a factor of two increase in stress, not a factor of 8. This implies that the strain rate of the composite is more complex than the simple addition of a parallel or series process.

Finally, and most puzzling, is that the presence of 40 vol.% Ni results in a threshold stress. Models of GBS have been proposed that employ a threshold stress.[27] In this case, σ_0 is the minimum stress to initiate grain-boundary sliding.

If we assume that the deformation of the composite is primarily via GBS, then what is the role of the Ni? Here, we adapt ideas from a recent model developed to describe tensile creep of Si_3N_4 containing a deformable second phase.[28] It should be cautioned, however, that the model may not be strictly applicable because both the ceramic and the Ni phase can deform.

The model predicts that as the ceramic grains slide, cavities form and the Ni, under a tensile stress, will move to fill the cavities. The viscosity of the Ni phase becomes important. The tensile stress will reduce the viscosity of the Ni phase. The viscosity will also depend on temperature: decreasing with increasing temperature as the Ni phase becomes more plastic. The recrystallization of Ni causes complications. There are three steps in the process outlined above: (1) GBS, (2) cavity formation, and (3) Ni flow via diffusion to fill the cavities. It is impossible at present to determine which step controls creep or even if they are independent and act in parallel or series steps, or are coupled in a complex manner.

These processes can be described by a general equation of the form

$$\dot{\varepsilon} = C\frac{\sigma}{\eta}, \tag{3}$$

where C is a constant and η is the viscosity of the Ni phase. The viscosity is given by

$$\eta = \eta_o \exp(Q/RT)\exp(\gamma/\sigma), \tag{4}$$

where η_o and γ are constants. The double exponential $\exp(Q/RT)\exp(\gamma/\sigma)$ accounts for the temperature and stress dependence of the viscosity of the Ni phase.

Eq. (4) can be substituted in Eq. (3) and the exponential expanded to first order to give, at a constant T,

$$\dot{\varepsilon} \propto \sigma(1-\gamma/\sigma). \tag{5}$$

Therefore, γ plays the role of a threshold stress and as γ increases so does the viscosity of the Ni phase, hence a higher stress will be required to "squeeze" the Ni phase into the cavities that would normally grow. The model can be checked for self-consistency because a plot of $\dot{\varepsilon}\exp(Q/RT)\exp(\gamma/\sigma)$ vs. σ should be linear. Such a plot has been made (Fig. 9) and is linear, as predicted. The single adjustable parameter is Q and the best fit yields $Q \approx 340$–360 kJ/mol in reasonable agreement with the value of 336 ± 43 kJ/mol calculated from Fig. 4. The regression coefficient is 0.96, considered very good considering the experimental uncertainty in the threshold stress data.

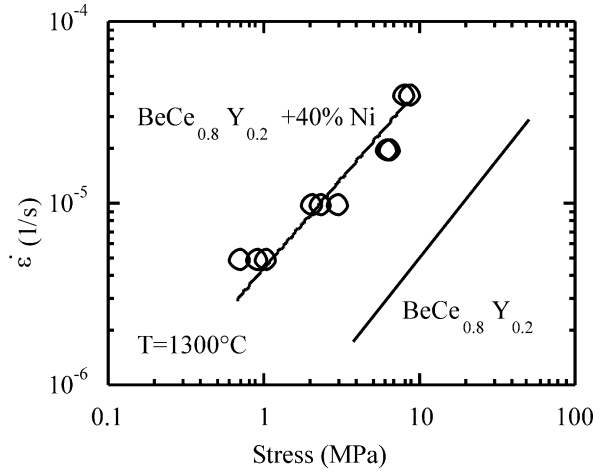

Fig. 8. Comparison of the creep rate of the composite $BaCe_{0.8}Y_{0.2}O_{3-y}+40\%$ Ni and the $BaCe_{0.8}Y_{0.2}O_{3-y}$ ceramic. Stress for the composite is $\sigma-\sigma_0$, while that for the ceramic is σ.

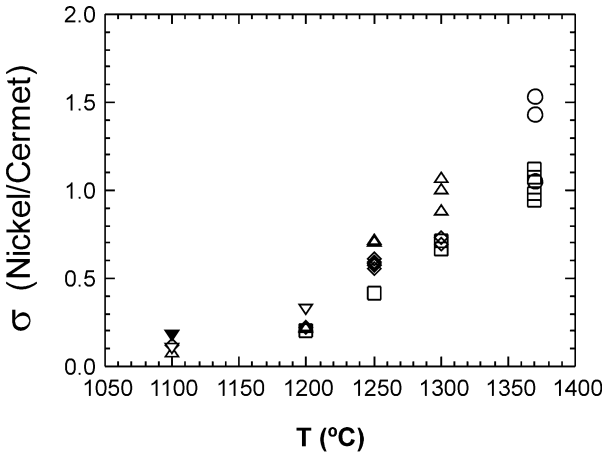

Fig. 10. Variation of the ratio of the steady-state stress of Ni 200 to that of the cermet $BaCe_{0.8}Y_{0.2}O_{3-y+40\%\ Ni}$. Symbols represent various strain rates: circles = 5 × 10–5 s^{-1}, squares = 4 × 10–5 s^{-1}, diamonds = 2 × 10–5 s^{-1}, triangles = 1 × 1–5 s^{-1}, inverted triangles = 5 × 10–6 s^{-1}, and inverted solid triangles = 2 × 10–6 s^{-1}.

The meaning of Q is not clear for several reasons. Should the data in Fig. 4 be corrected for load transferred to the Ni phase? Fig. 10 presents a plot of $\sigma_{cermet}/\sigma_{Ni}$ for various $\dot{\varepsilon}$ and T. It is noted that at 1370 °C the stresses become comparable. This suggests that the load transfer should be a function of temperature, adding further complications. Neglecting this point, the measured value of Q is higher than the activation energy for lattice self-diffusion of Ni reported to be 278 kJ/mol,[29] so that Q, if it represents a physical process, is probably not related to the deformation of Ni. The activation energy for creep of the composite could be related to the solubility of the ceramic in Ni, or to diffusive transfer of the ceramic through the Ni phase. If Q was related to the deformation of Ni or the solubility and subsequent diffusion through the Ni phase, the agreement between the Q for the composite and the ceramic would be entirely fortuitous. This leads us to believe that the deformation of BCY + Ni is controlled by GBS in the BCY ceramic and, therefore, the activation energy reflects the diffusion of one of the cations.

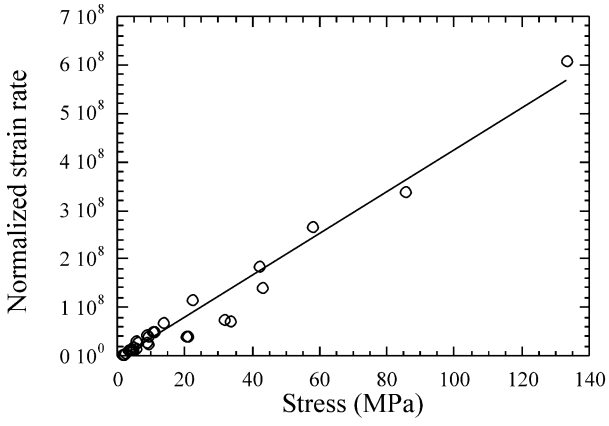

Fig. 9. Plot of normalized strain rate, $\dot{\varepsilon}\exp(Q/RT)\exp(\gamma/\sigma)$, calculated from the measured threshold stress and setting $Q = 360$ kJ/mol, vs. σ. The experimental points are shown.

5. Summary

The stress exponent and the activation energy for creep of $BaCe_{0.8}Y_{0.2}O_{3-y}$ and $BaCe_{0.8}Y_{0.2}O_{3-y}+40\%$ Ni are identical if one considers the existence of a threshold stress in the composite. These facts and the observations that the grain shape remains constant and no cavitation occurs imply that GBS is the deformation mechanism in the BCY ceramic. However, the addition of Ni to the ceramic results in a threshold stress and increases the creep rate eight fold. Moreover, the stress exponent remains unity and the activation energy for deformation of the composite remains the same as that of the ceramic. A model that assumes that the Ni phase is under a tensile stress in order to fill the cavities that result from GBS of the ceramic grains, based on a temperature- and stress-dependent viscosity, appears to fit the results.

Acknowledgements

This work was supported by the US Department of Energy, Federal Energy Technology Center, under Contract W-31–109-Eng-38; and by the Ministerio de Educación y Ciencias of Spain, under CICYT Project MAT97–0562-C02–01.

References

1. Iwahara, H., Esaka, T., Uchida, H. and Maeda, N., *Solid State Ionics*, 1981, **3/4**, 359.
2. Uchida, H., Maeda, N. and Iwahara, H., *J. Appl. Electrochem.*, 1982, **12**, 645.
3. Uchida, H., Maeda, N. and Iwahara, H., *Solid State Ionics*, 1983, **11**, 117.
4. Liang, K. C. and Nowick, A. S., *Solid State Ionics*, 1993, **61**, 77.
5. Nowick, A. S. and Du, Y., *Solid State Ionics*, 1995, **77**, 137.
6. Liu, J. F. and Nowick, A. S., *Mater. Res. Soc. Symp. Proc.*, 1991, **210**, 673.
7. Liu, J. F. and Nowick, A. S., *Solid State Ionics*, 1992, **50**, 131.
8. Bonanos, N., *Solid State Ionics*, 1992, **53–56**, 967.
9. Taniguchi, N., Hatoh, K., Niikura, J. and Gamo, T., *Solid State Ionics*, 1992, **53–56**, 998.
10. Bonanos, N., Ellis, B., Knight, K. S. and Mahmood, M. N., *Solid State Ionics*, 1989, **35**, 179.
11. Bonanos, N., *Phys. Chem. Solids*, 1993, **54**, 867.
12. Bausch, S., Bohn, H. G. and Schilling, W., *J. de Physique IV*, 1996, **6**, C8–695.
13. Reichel, U., Arons, R. R. and Schilling, W., *Solid State Ionics*, 1996, **86–88**, 639.
14. Kosacki, I. and Anderson, H. U., *Appl. Phys. Lett.*, 1996, **69**, 4171.
15. Guan, J., Dorris, S. E., Balachandran, U. and Liu, M., *Solid State Ionics*, 1997, **100**, 45.
16. Flint, S. D., Hartmanová, M., Jones, J. S. and Slade, R. C. T., *Solid State Ionics*, 1996, **86–88**, 879.
17. Iwahara, H., Yajima, T. and Ushida, H., *Solid State Ionics*, 1994, **70/71**, 267.
18. Goretta, K. C., Park, E. T., Guan, J., Balachandran, U., Dorris, S. E. and Routbort, J. L., *Solid State Ionics*, 1998, **111**, 295.
19. Park, E. T., Goretta, K. C., de Arellano-López, A. R., Guan, J., Balachandran, U., Dorris, S. E. and Routbort, J. L., *Solid State Ionics*, 1999, **117**, 323.
20. Guan, J., Dorris, S. E., Balachandran, U. and Liu, M., *Ceram. Trans.*, 1998, **92**, 1.
21. Guan, J. PhD thesis, Georgia Institute of Technology, 1998.
22. Takeuchi, K., Loong, C.-K., Richarsdon, J. W., Guan jr, J., Dorris, S. E. and Balachandran, U., *Sol. State Ionics*, 2000, **138**, 63.
23. Routbort, J., *Acta Metall.*, 1979, **27**, 649.
24. Cannon, W. R. and Langdon, T. G., *J. Mater. Sci.*, 1983, **23**, 1.
25. Weertman, J. and Shaninian, P., *Trans. AIME*, 1956, **206**, 1223.
26. Kingery, W. D., Bowen, H. K. and Uhlmann, D. R., *Introduction to Ceramics*. John Wiley & Sons, New York, 1976.
27. Ashby, M. F. and Verrall, R. A., *Acta Metall*, 1973, **21**, 149.
28. Luecke, W. E. and Wiederhorn, S. M., *J. Am. Ceram. Soc.*, 1999, **82**, 2769.
29. Bakker, H., *Phys. Stat. Sol.*, 1968, **28**, 569.